Phospholipid Species Act as Modulators in p97/p47-Mediated Fusion of Golgi Membranes †

ARTICLE *in* BIOCHEMISTRY · SEPTEMBER 2002

Impact Factor: 3.02 · DOI: 10.1021/bi0259195 · Source: PubMed

6 AUTHORS, INCLUDING:

Olaf Maier
Universität Stuttgart
32 PUBLICATIONS **753** CITATIONS
SEE PROFILE

Udo Bakowsky
Philipps University of Marburg
129 PUBLICATIONS **4,927** CITATIONS
SEE PROFILE

Jean-Marie Ruysschaert
Université Libre de Bruxelles
472 PUBLICATIONS **13,872** CITATIONS
SEE PROFILE

Phospholipid Species Act as Modulators in p97/p47-Mediated Fusion of Golgi Membranes†

Eve-Isabelle Pécheur,[‡,¶,#] Isabelle Martin,[§,#] Olaf Maier,[‡] Udo Bakowsky,[‡] Jean-Marie Ruysschaert,[§] and Dick Hoekstra*[,‡]

Department of Membrane Cell Biology, University of Groningen, Antonius Deusinglaan 1, 9713 AV Groningen, The Netherlands, and Laboratoire des Macromolécules aux Interfaces, Université Libre de Bruxelles, Bvd du triomphe, B-1050, Brussels, Belgium

Received April 4, 2002; Revised Manuscript Received May 30, 2002

ABSTRACT: The ATPase p97 in complex with p47 participates in Golgi cisternae rebuilding after mitosis. In a Golgi-liposome assay, the complex triggered a phosphatidylethanolamine (PE)-promoted fusion. Here we show for the first time that fusion between mitotic Golgi membranes induced by adding cytosol or purified p97/p47 is modulated by PE present in Golgi membranes. Using model membranes, we demonstrate a PE-dependent recruitment of p97/p47 to membranes, causing dramatic conformational rearrangements and favoring protein−lipid interactions. Previously buried hydrophobic sites become exposed in a controlled manner, which leads to the penetration of (a) domain(s) of the complex into lipid bilayers, facilitated by a PE-dependent increase in headgroup spacing. In contrast, when facing phosphatidylcholine (PC) the complex clusters extensively. This implies that in the presence of PC protein−protein interactions rather than fusion-promoting protein−lipid interactions occur. Importantly, PE-mediated changes in secondary and tertiary structures are exclusively observed when p97 is complexed with p47, which is a prerequisite for membrane fusion. We therefore propose that at physiological conditions PE-induced conformational changes in p97/p47 are relevant in triggering this activity.

The reassembly of Golgi cisternae after pharmacological or physiological vesiculation (e.g., mitosis) requires two distinct fusion machineries (*1*, *2*). Both include the cytosolic ATPases *N*-ethylmaleimide sensitive factor (NSF) and p97 in complex with their respective cofactors, α-SNAP and p47, which associate with the same t-SNARE (target SNAP REceptor)[1] at the Golgi membrane syntaxin 5 (*3*). These fusion machineries differ in the way they interact with their cofactor and in terms of the morphology of their fusion end-products. In Golgi assembly, the NSF pathway reconstitutes the (highly curved) rims, whereas the p97 pathway rebuilds the (flattened) core of a Golgi cisterna (*4*). NSF forms a complex with α-SNAP only when the cofactor is membrane-associated (*5*). Also, the membrane binding properties of α-SNAP depend on the type of membrane. Thus, its binding to Golgi membranes requires the presence of functional SNAREs, while SNAREs are not needed for its binding to brain membranes (*6*). In contrast, p97/p47 can be isolated as a stable cytosolic complex (*7*), but its mode of interaction with membranes is unclear. α-SNAP and p47 compete for binding to syntaxin 5 on Golgi membranes, thereby directing the preferential binding of NSF or p97, respectively. Since α-SNAP and p47 share some sequence homology and are found in similar amounts in the cytosol (*3*), a similarity in membrane association of either complex is plausible, p47 providing a "membrane-anchoring site" for p97. Interestingly, recent evidence revealed that p47 competes with Ufd1/Npl4 for binding to p97 in the Golgi, p47 directing p97 into postmitotic Golgi membrane fusion, whereas Ufd1/Np14 leads p97 in ubiquitin-dependent events during mitosis, respectively (*8*). Protein/protein interactions are therefore relevant to the overall fusion mechanism involving either the p97/p47 complex (*3*, *8*) or the yeast p97 homologue, cdc48p (*9*). However, a role of *direct* protein/lipid interactions, the ultimate requirement in triggering fusion, has not yet been fully explored. Recently, the fusion capacity of the p97/47 complex has been reconstituted in a pure liposomal membrane system, and it was shown that phosphatidylethanolamine (PE)-containing membranes strongly promote membrane fusion (*10*). This finding prompted a reconsideration of the previously claimed direct involvement of SNAREs in causing membrane fusion (*11*), particularly in light of the gradually accumulating evidence that supports *trans*-v-t-SNARE pairing as a specific targeting step that precedes but does *not* participate in the actual fusion event (*12*−*15*), and

† This work was supported by the European Commission (D.H.), the "Akademie Deutscher Naturforscher Leopoldina" (U.B. and O.M.), and the Action de Recherches Concertées (J.M.R.).

* Corresponding author. Dept of Membrane Cell Biology, University of Groningen, Antonius Deusinglaan 1, 9713 AV Groningen, The Netherlands. Tel: 31-50-363-2741. Fax: 31-50-363-2728. E-mail: d.hoekstra@med.rug.nl.

# These authors contributed equally to this work.

‡ University of Groningen.

§ Université Libre de Bruxelles.

¶ Present address: UMR 5086 CNRS, IBCP, 7 passage du Vercors, 69367 Lyon Cedex, France.

[1] Abbreviations: PC, PE, PS, PI, phosphatidylcholine, -ethanolamine, -serine, -inositol; TNBS, trinitro-benzene sulfonic acid; NEM, *N*-ethylmaleimide; *S*-Ado-Met, *S*-adenosyl methionine; MGF, mitotic Golgi fragments; DTT, dithiothreitol; ATR-FTIR, attenuated total reflection Fourier transform infrared spectroscopy; AFM, atomic force microscopy.

10.1021/bi0259195 CCC: $22.00
Published on Web 07/10/2002

in light of recent work that NSF has a role in Golgi membrane fusion separate from its ability to disassemble SNARE complexes (*16*).

The present work was undertaken to investigate the physiological relevance and mechanism of the prominent PE-dependence of p97/47-induced membrane fusion, prompted by our previous observations in a reconstituted p97/p47 system (*10*). To this end, we have reconstituted fusion in a pure biological system between mitotic Golgi fragments (*2*) using an assay that allows sensitive and continuous monitoring of membrane merging. In this biological assay, we show that PE indeed regulates p97/p47-mediated Golgi membrane fusion. In model membrane studies, we then demonstrate that PE induces conformational rearrangements in the secondary and tertiary structures of the complex, which can be correlated with its fusion potency. By contrast, when facing PC protein−protein interactions are favored, which abrogates the fusion potency of the p97/p47 complex.

MATERIALS AND METHODS

Chemicals. Lipids were purchased from Avanti Polar Lipids. 1-Oleoyl-2-[6-(7-nitro-2,1,3-benzoxadiazol-4-yl)amino]hexanoyl phosphatidylcholine (C_6-NBD-PC), [4,4′-bis-(anilino-8 naphthalenesulfonate)] (bisANS), N-NBD-PE, N-Rh-PE, and octadecylrhodamine (R18) were from Molecular Probes. Hydrazine was from Merck, trinitrobenzene sulfonic acid (TNBS), calcein, and *N*-ethylmaleimide (NEM) were from Sigma, and *S*-adenosyl-l-[methyl-^{14}C]methionine (*S*-Ado-Met, 62 mCi/mmol) was from Amersham Pharmacia Biotech. L-Lactic dehydrogenase (LDH) from rabbit muscle was from Roche (Mannheim, Germany). p97/p47 was purified according to Otter-Nilsson et al. (*10*), and purity of the complex was checked after silver staining of SDS−PAGE gels. This revealed the absence of additional proteins. A monoclonal antibody to p97 was purchased from Progen Biotechnik. Polyclonal antibodies to p47 were obtained from Syntem S. A. (Nîmes, France).

Preparation of Liposomes and Mitotic Golgi Membranes. Liposomes (100 nm) were prepared from brain or synthetic (dioleoyl form) phospholipids as described (*10*). Rat liver Golgi stacks were prepared according to Slusarewicz et al. (*17*) and incubated with mitotic cytosol prepared from HepG2 cells, as described (*18*), to give mitotic Golgi fragments (MGF) (*2*). Fragmentation was checked by electron microscopy as described (*2*).

Lipid Binding Assay. Rat liver cytosol (8 mg/mL final) or purified p97/p47 (20 μg) were incubated with 400 μg of lipid vesicles for 1 h at 37 °C in 400 μL of "fusion" buffer (20 mM Hepes, 150 mM KCl, 10 mM KOAc, 1 mM $MgCl_2$, and 1 mM ATP, pH 6.8). In the case of purified complex, the final molar protein/lipid ratio was 1:19 000. Lipid binding was assayed after fractionating on linear 3−40% sucrose gradients, centrifuged at 100000*g*, 4 °C for 16 h. Five hundred microliter fractions were collected, analyzed for lipid phosphorus, and submitted to trichloroacetic acid protein precipitation. Pellets were resuspended in SDS sample buffer, and analyzed by SDS−PAGE, followed by silver-staining or immunoblot.

PE Conversion on Golgi Membranes and Fusion Assay. PE was converted to trinitrophenyl-PE (TNP-PE) by treatment with TNBS (*19*), or to phosphatidylcholine (PC) by methylation via Golgi PE *N*-methyltransferase (*20*). MGF were treated with 2.5 mM NEM for 15 min on ice (to prevent reassembly), and quenched by 5 mM DTT (*2*). A fraction was labeled with R18 (15 nmol/mg of protein) for 30 min on ice, and unincorporated fluorophore was removed by centrifugation (donor membranes). Another fraction was resuspended either in 40 mM $NaHCO_3$, 120 mM NaCl, and 5 mM glucose, pH 8.6, and incubated 1 h at 30 °C with 3 mM TNBS, or in 125 mM Tris-HCl, 5 mM DTT, pH 9.2, and incubated for 10 min at 37 °C with 200 μM [methyl-^{14}C]*S*-AdoMet. Conversion of PE to TNP-PE or PC was analyzed by two-dimensional high-performance thin-layer chromatography (2D-HPTLC), after lipid extraction. After a 1-h treatment of mitotic Golgi fragments with 3 mM TNBS, the *total* (cytosolic + lumenal) amount of PE is reduced by 3-fold as compared to control fragments. Reconversion of TNP-PE to PE was done by incubating the membranes 30 min with 2 mM hydrazine at 30 °C (*21*). After incubation of Golgi membranes with [methyl-^{14}C]*S*-Ado-Met, radioactivity was merely incorporated into PC.

Fusion between donor and acceptor membranes (12.5 μg each) was initiated by addition of rat liver cytosol (8 mg of protein/mL final) or purified p97/p47 (300 μg/mL final), in 1 mL of fusion buffer equilibrated at 37 °C, supplemented with an ATP regenerating system (1 mM ATP, 40 mM creatine phosphate, and 0.2 mg/mL creatine phosphokinase). R18 fluorescence dequenching was followed at 560 nm (excitation) and 590 nm (emission) (*24*).

Fluorescence Spectroscopy. (a) Determination of Headgroup Spacing. Lipid headgroup spacing in the liposomal bilayers of different composition was determined by using C_6-NBD-PC (*22*), as described previously (*23*). Briefly, the lipid analogue readily incorporates into liposomes from micelles (where self-quenching is 100%). After a 10-min equilibration period at 37 °C in the presence of 1 mol % C_6-NBD-PC (final concentration), the fluorescence is measured at $\lambda_{exc} = 460$ nm and $\lambda_{em} = 534$ nm. The fluorescence of C_6-NBD-PC depends on the facility for the fluorophore to intercalate into the lipid hydrocarbon core, and is a function of the degree of hydration of the polar headgroups, as a reflection of headgroup spacing. Note that all measurements were done in the absence of rat liver Golgi membranes.

(b) Labeling of Proteins with bisANS. Samples containing 60 μM bisANS and 6 nM p97/p47 in fusion buffer were excited at 365 nm, and fluorescence emission spectra were recorded between 400 and 620 nm in an SLM SPF-500C spectrofluorimeter, as described (*24*). Other experimental conditions are described in the figure legend.

(c) Tryptophan Fluorescence Quenching. Trp fluorescence measurements ($\lambda_{exc} = 295$ nm, $\lambda_{em} = 340$ nm) were done in the absence or presence of lipid vesicles, with increasing amounts of acrylamide (which acts as an aqueous collisional quencher of Trp). Data were corrected for vesicle-induced light scattering and dilution. The quenching data were analyzed by the Stern−Volmer plot, as described (*23*).

(d) Fluorescence Assay for Fusion. Bilayer mixing (at 37 °C) was assayed through resonance energy transfer (*24*). For Golgi−liposome fusion, rat liver Golgi membranes (50 μg of protein), prepared as described (*10*), were added to a suspension of liposomes labeled with 1 mol % each of *N*-NBD-PE and *N*-Rh-PE, in a final volume of 1 mL of fusion buffer. The 100% fluorescence was determined after

adding Triton X-100 (0.1% final) to the suspension, and was corrected for dilution and detergent-quenching. The 0% level corresponds to the fluorescence reading of the initial vesicle population.

(e) Fluorescence Assay for LDH Leakage. Calcein was encapsulated into liposomes by hydrating the lipid film (PC/PE/PS, 3:3:1, 2.5 mM final) in buffer A, containing 80 mM calcein, 150 mM NaCl, 10 mM Hepes, 1 mM EDTA, pH 7.4. Liposomes were then prepared as described above, and unencapsulated calcein was removed by gel filtration over a Sephadex G-50 column equilibrated with buffer A. The leakage assay was performed in buffer A with 10 μM calcein-loaded liposomes, in the presence of 10 μg/mL LDH. Fluorescence signal was followed at $\lambda_{exc} = 495$ nm and $\lambda_{em} = 515$ nm. Fluorescence data were normalized by setting the initial fluorescence intensity of calcein-loaded liposomes to zero, and the intensity of dequenched fluorophore obtained after lysis of the liposomes with Triton X-100 (0.5% v/v) to 100.

Attenuated Total Reflection Infrared (ATR-FTIR) Spectroscopy Measurements. Oriented multilayers were obtained by slow evaporation of the lipid vesicles incubated with p97 or p97/p47, under an N_2 stream at room temperature on one side of the germanium plate, which is the internal reflection element (50 × 50 × 2 mm, Harrick EJ2121) with an aperture angle of 45°, yielding 25 internal reflections (*25*). For each FTIR spectrum, 512 scans were then recorded at room temperature on a Bruker IFS55 FTIR spectrophotometer equipped with a liquid nitrogen-cooled mercury cadmium telluride detector at a nominal resolution of 4 cm^{-1}. For the deuteration kinetics, samples were spread on the germanium plate, and 10 spectra were recorded by ATR-FTIR to verify the reproducibility of the measurements and stability of the system. Spectral analysis of the amide I and II band areas were carried out as previously described (*23*, *26*).

The ATR-FTIR conformation analysis was performed on the amide I region of deuterated samples, located in a region of the spectrum often free of other bands and composed of 80% pure C═O vibration as described (*23*, *25*).

Polarized ATR-FTIR spectroscopy was used to determine the orientation of the lipid membrane. The symmetric (ν_{sym} (CH_2) ~ 2850 cm^{-1}) and the antisymmetric ($\nu_{antisym}$ (CH_2) ~ 2920 cm^{-1}) vibrations of the lipid methylene CH bonds are perpendicular to the molecular axis of a fully extended hydrocarbon chain. Thus, measurements of the dichroism of infrared light absorbance can reveal the order and orientation of the membrane sample relative to the crystal. Polarization was expressed as the dichroic ratio R_{ATR}, which equals $A_{90}°/A_0°$. The orientation order parameter f was calculated from R_{ATR} as described (*27*).

Atomic Force Microscopy. Lipids, dissolved in $CHCl_3$/CH_3OH (2:1, v:v), were spread at the air/water interface of a Wilhelmy balance system (R&K GmbH, Mainz, Germany), and the lipid film was equilibrated 10 min to 0 mN/m. Films were then compressed stepwize, up to a surface pressure of 20 mN/m. Two micrograms of purified p97/p47 were then injected into the subphase. Lipid membranes, following p97/p47 adsorption and transfer onto silicon wafers, were visualized by atomic force microscopy (AFM Nanoscope III dimension 5000, Digital Instruments, Santa Barbara, CA) under fully hydrated conditions (*28*) at 25 °C.

RESULTS

PE Mediates p97/p47-Induced Homotypic Fusion between Golgi Membranes. It was shown previously that p97/p47 induces rapid membrane fusion in an ATP-dependent manner (*10*). Importantly, the unambiguous occurrence of genuine membrane fusion in this assay was revealed by demonstrating both lipid *and* contents mixing, which proceeded with virtually identical kinetics. Both liposome−liposome and liposome−Golgi fusion could be reconstituted, occurring on a time scale of min, and PE in particular promoted the merging event. Importantly, the exclusiveness of p97/p47 as the cytosolic fusogen was revealed by demonstrating that upon depletion of p97 from the cytosol fusion was inhibited by more than 80% (*10*). To appreciate the *biological relevance* of such observations, we applied an assay based upon lipid mixing (*24*) to monitor fusion between mitotic Golgi fragments (MGF), and devised protocols to modify their cytoplasmic pool of PE. Note that in contrast to the reconstituted p97/p47 system (*10*) contents mixing cannot be monitored in this case. We therefore performed control experiments to exclude that lipid mixing as a measure of fusion occurred as a result of probe transfer. When mixing unlabeled (acceptor) membranes with R18-labeled MGF in buffer, no lipid mixing was observed (Figure 1A, curve d; Figure 1B,C, curves c). However, fusion was readily triggered upon addition of cytosol or purified p97/p47 complex (Figure 1, curve a). Inclusion of calcium chelators in the fusion medium did not affect the fusion reaction (not shown). Using this assay, two experimental approaches were taken to investigate the PE-dependence of Golgi membrane fusion. In the acceptor membranes, the pool of PE was modified by (i) chemical treatment with TNBS, leading to the conversion of PE into TNP-PE, and (ii) by enzymatic conversion of PE into PC. A 1-h treatment with TNBS inhibited Golgi membrane fusion by ca. 50% (Figure 1A, curve b). Inhibition was proportional to the incubation time with TNBS, resulting in an inhibition by 70% after 90 min (data not shown) and 100% after a treatment of 120 min (Figure 1A, curve e). Importantly, in all cases, fusion was restored upon reconverting TNP-PE into PE with 2 mM hydrazine (Figure 1A, curve c). Control levels of fusion were obtained when acceptor membranes were incubated for 2 h in the TNBS reaction buffer, and TNBS per se did not interfere with R18 fluorescence. Also, hydrazine did not affect cytosol-induced fusion (Figure 1A, similar curve as curve a).

Trinitrophenylation with TNBS can occur on primary amino groups of lysine residues in proteins, and on amino groups in aminophospholipids such as PE and phosphatidylserine (PS). The extent of chemical modification of protein lysine residues is difficult to predict, and such residues may in fact not be modified at all (*29*). However, hydrazine treatment can restore the biological activity of the protein (*30*). Furthermore, we observed a weak TNP-derivatization on PS by thin-layer chromatography (data not shown). Therefore, the exclusiveness of a PE-dependent effect was further investigated by taking advantage of the presence of an isoform of the PE *N*-methyl transferase on rat liver Golgi membranes (*20*). Thus, by adding a methyl group donor (*S*-Ado-Met) to the Golgi membranes, PE-*N*-methyltransferase activity localized at its cytosolic leaflet converts PE into PC (*20*, and data not shown). Indeed, after

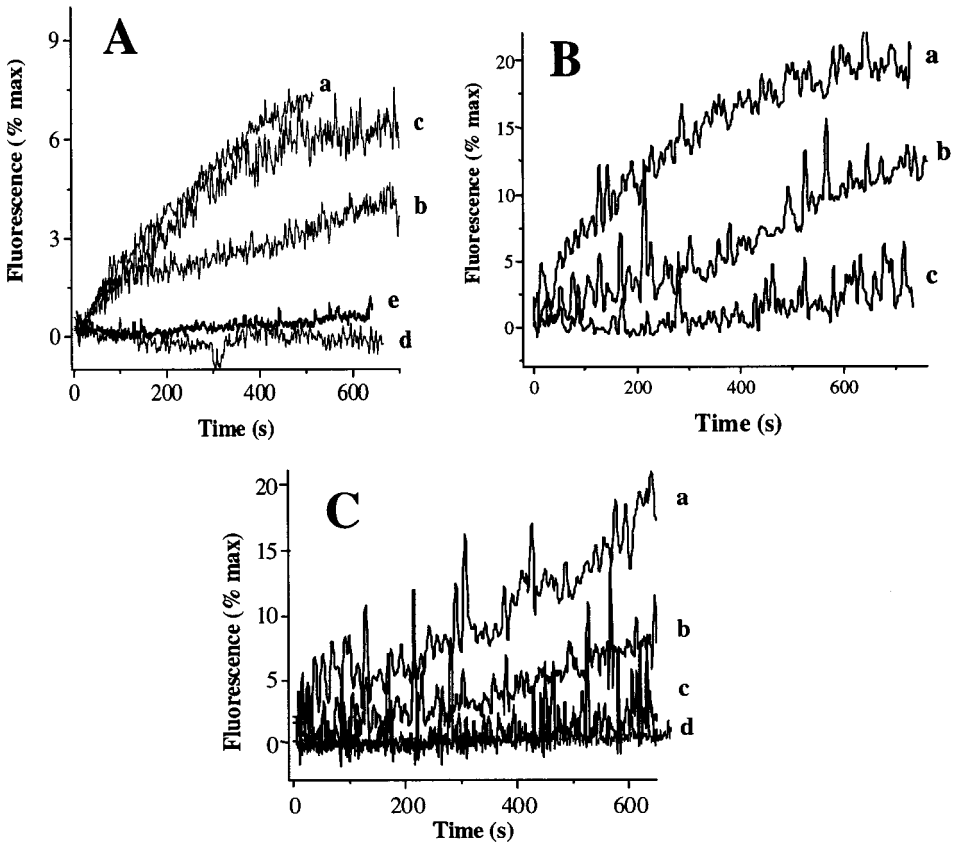

FIGURE 1: Golgi membrane fusion depends on PE. Panel A, NEM-treated MGF are incubated 1 h with 3 mM TNBS to convert PE into TNP-PE. They are then mixed with NEM-treated and R18-labeled MGF (12.5 μg each) at 37 °C in "fusion buffer" pH 6.8. Fusion is initiated by adding cytosol (8 mg/mL final) (curve b). a, control without TNBS treatment; d, control without cytosol; e represents fusion observed after a 2-h incubation with TNBS. c, Golgi fusion after reconversion of TNP-PE to PE (see Methods). Panel B, Acceptor membranes are incubated with [^{14}C]*S*-Ado-Met at 37 °C, to convert the cytosolic PE pool into PC. Fusion is then recorded as above (curve b). a, control: without *S*-Ado-Met/with "donors", incubated 10 min in buffer pH 9.2, or with *S*-Ado-Met in buffer pH 9.2/with "acceptors" at $T = 0$ after addition of *S*-Ado-Met. c, control after treatment with *S*-Ado-Met without cytosol. Panel C, fusion between MGF is initiated with purified p97/p47 (final 300 μg/mL, i.e., 405 pmol/mL) (curve a). b, acceptor MGF treated with *S*-Ado-Met; c, control without p97/p47; d, fusion observed with LDH (final 100 μg/mL, i.e., 2700 pmol/mL). Curves are representative of three separate experiments.

a 10-min incubation of acceptor Golgi membranes with [^{14}C]-labeled *S*-Ado-Met, radioactivity was only incorporated into PC, and as a consequence, we observed that cytosol- or p97/p47-induced Golgi fusion was reduced by 2-fold as compared to control (Figure 1B,C, curve b). Control fusion levels (curve a) were obtained when acceptor membranes were collected immediately after addition of *S*-Ado-Met (T_0), or when donor membranes were incubated for 10 min in reaction buffer.

To further investigate the observed PE specificity, we took into account a recent claim that certain proteins not relevant to physiological fusion processes readily trigger lipid mixing in a liposome−liposome assay, facilitated by PE (*31*). To exclude nonspecificity, we used one of these proteins, lactic dehydrogenase (LDH), in several of our assays and determined its fusion capacity. Not unexpectedly (see Discussion), LDH induced lipid mixing in the liposome−liposome assay, using vesicles composed of PC/PE/PS (3:3:1) (data not shown). However, extensive calcein leakage was concomitantly observed (approximately 10%/min), indicating a poor level of control of the lipid destabilization process (data not shown). Conversely, as reported in detail previously (*10*), p97/p47 in a similar assay is essentially nonleaky reflecting a genuine fusion event. We then investigated the effect of LDH in our Golgi−Golgi assay. As clearly shown in Figure 1, whereas only 405 pmol/mL p97/p47 gives rise to dequenching (i.e., 300 μg/mL) (Figure 1C curve a), no dequenching signal is observed with LDH over the entire time period (curve d), even when a 6-fold higher protein concentration was used (2700 pmol/mL, i.e., 100 μg/mL). This clearly indicates that although LDH is able to induce lipid mixing, its features otherwise completely differ from those observed for the p97/p47 complex, and it does not induce any fusion in a biologically relevant assay for Golgi−Golgi fusion (Figure 1C).

Taken together, these data demonstrate that p97/p47-induced fusion of Golgi membranes in a pure biological assay displays a pronounced dependence on PE, thus corroborating and extending previous data obtained in a (semi-)artificial system (*10*). Although negative bilayer curvature-promoting properties, which stimulate membrane fusion, may underlie the facilitating effect of PE (*10*, *23*), effects of PE on both bilayer properties and protein structure are possible. Accordingly, we then examined in detail the interaction of p97/p47 with membranes of various compositions, first focusing on the ability of the complex to associate with membranes as a function of PE content.

p97/p47 Associates with PE-Containing Liposomes. We investigated the interaction of p97/p47, from rat liver cytosol or as purified complex, with liposomes prepared from the major phospholipids [i.e., phosphatidylcholine (PC), phos-

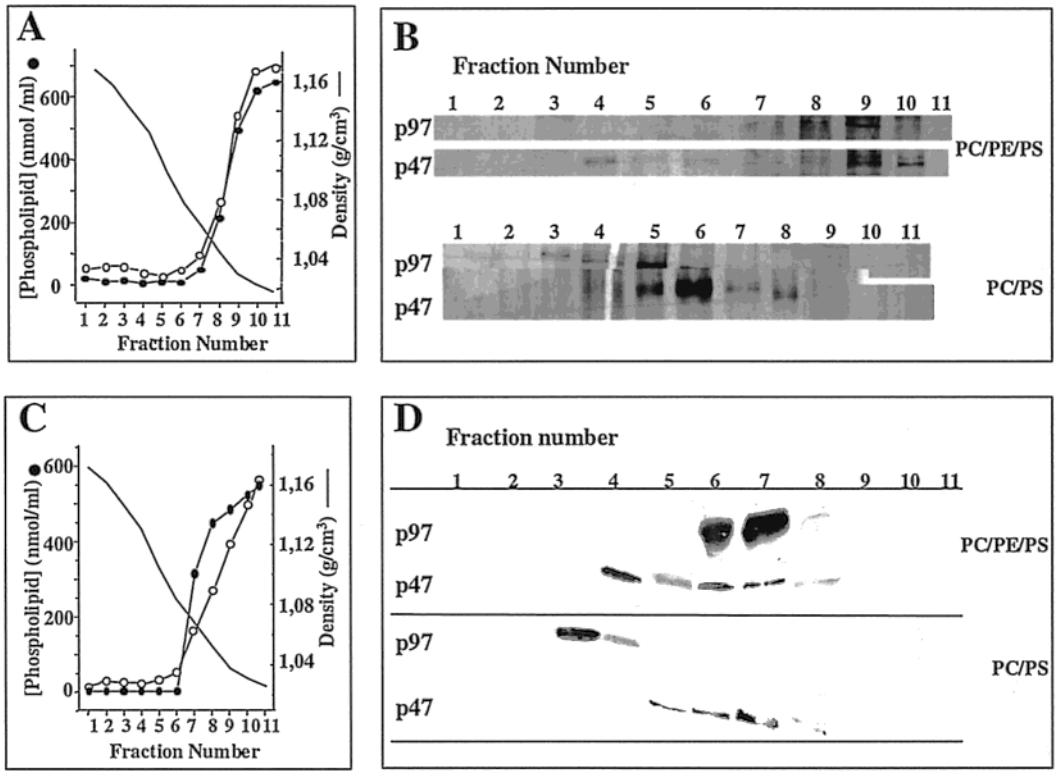

FIGURE 2: p97/p47 lipid association depends on the presence of PE. Purified p97/p47 (A, B) (final molar protein-to-lipid ratio 1:19 000) or rat liver cytosol (C, D) are incubated 1 h with liposomes of DOPC/DOPS/DOPE (molar ratio 5.2:1.2:3.6, closed symbols in panels A and C) or DOPC/DOPS (8.8:1.2, open symbols in panels A and C). After fractionation by density gradients (A, C), samples are analyzed by SDS−PAGE after silver staining (B), or by immunoblotting with anti-p97 and -p47 antibodies (D). Note that similar results are obtained with brain PC, PS, and PE.

phatidylserine (PS), phosphatidylinositol (PI), and PE] localized at the cytosolic leaflet of the mammalian Golgi membrane (*32*). After a 1-h incubation at 37 °C, the liposome mixture was fractionated by density gradient centrifugation. Liposomes were recovered on top (fractions 8−11, Figure 2A and C, closed symbols for PC/PE/PS; open symbols for PC/PS), and the unbound protein complex in fractions 3−6. As shown in Figure 2B (purified complex) and 2D (cytosol), p97/p47 associates with vesicles containing brain PE or dioleoylPE, as in PC/PS/PE (Figure 2B,D) or PC/PE (not shown), but *not* with those devoid of PE, such as PC/PS (Figure 2B,D). The presence of PI did not modify or improve this recruitment (not shown). Note that in the absence of liposomes, proteins would be recovered in fractions 3 to 5 (data not shown). Interestingly, p97 displays an exclusive and high affinity for PE-containing bilayers, since little if any "free" protein is detected in the gradient. Also, the relative amount of p97 bound to PE-containing bilayers consistently exceeds that of p47 present in the same liposomal fraction. By contrast, p47 shows a less pronounced lipid specificity, reminiscent of that of α-SNAP (*6*). However, the association of p47 with membranes is not strictly required for recruiting and/or stabilizing the interaction with p97, since addition of p97 alone also leads to an efficient association with PE-containing vesicles (Figure 3). Yet, it should be emphasized that the p97/p47 *complex* is required for triggering fusion of vesicles of identical composition (inset, Figure 7) (*10*).

Headgroup spacing is an important parameter that may modulate the surface properties of a membrane, and thereby its susceptibility to protein-induced fusion. As demonstrated

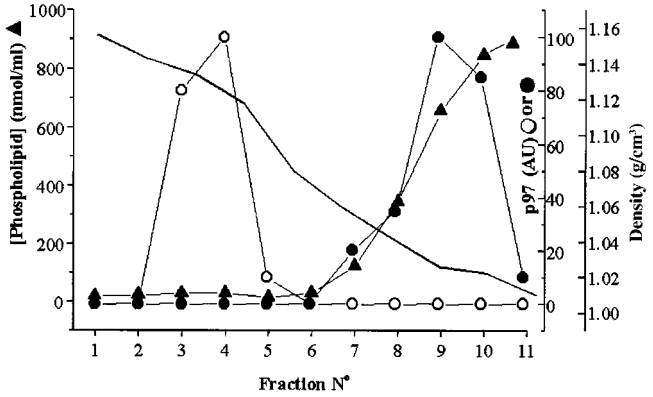

FIGURE 3: PE promotes the association of p97 to liposomes. p97 was incubated for 1 h with liposomes, with (PC/PS/PE, ●) or without PE (PC/PS, ○). After gradient fractionation, fractions were collected and analyzed by SDS−PAGE and silver staining for protein and lipid content (▲). p97 bands on gels were scanned and analyzed by densitometry (○, ●). The density profile is indicated as a straight line.

elsewhere (*33*), spacing may facilitate (peptide) penetration, a putative crucial step in the mechanism of protein-induced fusion. To examine the role of this parameter in facilitating the preferential association of the p97/p47 complex with the PE-containing bilayers, the next experiments were carried out.

Headgroup Spacing and Membrane Surface Distribution of p97/p47 Are PE-Dependent. When plotting the headgroup spacing of various liposomal bilayers used in the present study, and their fusion activity, the correlation between initial rates of fusion and PE-modulated headgroup spacing, as

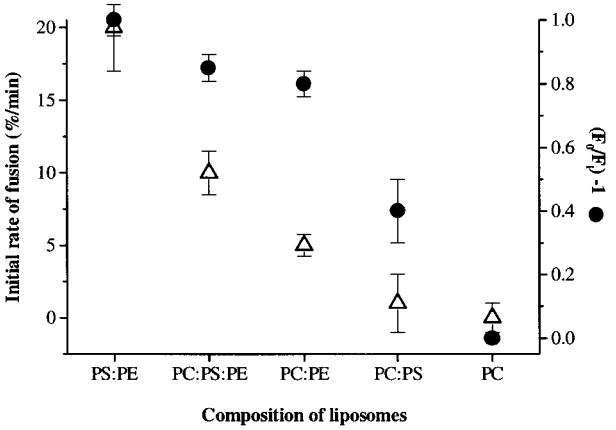

FIGURE 4: p97/p47-induced fusion correlates with target membrane headgroup spacing. Fusion between Golgi membranes and fluorescently labeled liposomes is monitored and the initial rates of fusion calculated (△). Headgroup spacing (●) in target liposomes is assessed as outlined in Methods. The fluorescence intensity (F_i) was recorded and normalized to the value for PC vesicles (F_0). Results are then expressed as (F_0/F_i) − 1, and represent the mean of three separate experiments (± SEM).

Table 1: Initial rates of fusion between rat liver Golgi membranes and liposomes of indicated lipid composition

composition	initial rate of fusion[a] (%/min)
PC	0
PC/PS 1:1	0.6
PC/PE 1:1	3
PC/PS/PE 1:1:1	7.3
PS/PE 1:1	18.6

[a] Initial rates of fusion (error is within 10%) were obtained from the steepest part of fusion curves recorded between rat liver Golgi membranes (50 μg of protein/assay) and liposomes (100 μM lipid, final concentration), in "fusion buffer" pH 6.8 (see Materials and Methods), as described (*10*).

apparent in the various liposomal bilayers used in this study, is striking (Figure 4). PE displays a spacing effect (compare PC and PC/PS with PE-containing vesicles), most likely due to its principle molecular shape as an inverted cone (*22*). This relates well to an increase in fusion susceptibility (Figure 4, Table 1). Interestingly, PS also exhibits spacing properties (compare PC with PC/PS vesicles), but this feature is not translated into a functional consequence, i.e., fusion (Table 1), as anticipated, since negligible membrane association of the complex is seen in the absence of PE (Figure 2; see above). Therefore, these results further support the view that PE represents a determining parameter in creating optimal conditions for p97/p47-mediated fusion.

Accordingly, it is tempting to suggest that the increase in lateral spacing may therefore facilitate the interaction with and/or the insertion of (a) domain(s) of p97/p47 into the target bilayer. To further define the nature of the interaction of the protein complex with target membranes, we then studied by microscopy the protein's interaction with monolayers and vesicles, composed of PE/PS or PC, which gave the most extreme outcome in terms of fusion susceptibility, the former showing the highest and the latter the lowest activity (Table 1, Figure 4). As shown in Figure 5, analysis by atomic force microscopy reveals the presence of large clusters of p97/p47 in association with the PC monolayer (picture III), whereas a homogeneous distribution is seen on the PE/PS film (picture I). Essentially the same phenomena are observed when p97/p47 interacts with either PE/PS or PC vesicles, as visualized by electron microscopy (pictures II and IV, respectively). Intriguingly, when substituting PS for PC in the PE/PS vesicles, a transitional picture emerged, showing both evenly dispersed proteins as well as clusters (data not shown). Hence, the data suggest that PE promotes the interaction of p97/p47 with the membrane surface, which leads to a more subtle interaction with PE-containing than with PE-devoid membranes, involving protein−lipid rather than protein−protein (clustering) interactions (see also below). Indeed, the stimulatory effect of PE in p97/p47 complex interactions with membranes is further emphasized by the notion that PC/PE vesicles are fusogenic, PC/PS vesicles revealing less than half this activity, whereas no fusion is observed with PC vesicles (Figure 4; Table 1). A potential explanation for these observations could be that the interaction of p97/p47 with the PC bilayers triggers conformational changes that lead to the observed protein−protein interactions. It is likely that the aggregates thus formed show a diminished binding affinity and readily dissociate from the membrane, as reflected by the presence of protein aggregates near the vesicles rather than being attached (Figure 5). Accordingly, the data would suggest that upon interaction with PC protein−protein interactions are favored, whereas protein−lipid interactions prevail when the p97/p47 complex interacts with PE-containing membranes. Whether lipid-induced changes in protein structure could indeed underlie such differences in interaction was further examined.

Induction of Lipid-Specific Conformational Changes in p97/p47. BisANS is nonfluorescent in aqueous environments, but becomes strongly fluorescent when it binds to hydrophobic sites in proteins, rather than lipid vesicles (*34*). An emission shift toward lower wavelengths (blue shift) is observed when p97/p47 is added to bisANS, indicating the presence of hydrophobic pockets in the complex (Figure 6A, curve b). A further 25-nm blue shift is observed upon addition of lipid vesicles to the mixture of p97/p47 and bisANS. Note that in the presence of lipid vesicles alone, no significant change in the bisANS emission spectrum occurs (data not shown). Interestingly, the enhancement in the number of bisANS binding sites and/or the increase in quantum yield of bound probe molecules (both reflecting an increment in hydrophobic interaction sites) was much more pronounced for PC (curve e) than for PC/PS (curve d) or PE/PS liposomes (curve c). These data are entirely consistent with the microscopic observations (Figure 5) described in the previous section, implying that a much more subtle change in overall structure of the complex in terms of a change in "exposed" hydrophobicity is triggered when interacting with negatively charged PE-containing than with zwitterionic vesicles. Additional support for the lipid-dependent subtlety in driving p97/p47 complex conformational changes was derived from experiments in which the change in Trp fluorescence by the aqueous quencher acrylamide was monitored, as a measure of the "average" environment around the entire protein. As shown in Figure 6, relative to its environment in aqueous solution, p97/p47 faces a more hydrophilic environment after its interaction with PE/PS vesicles, whereas it faces a more hydrophobic environment after interacting with PC vesicles (Figure 6B). These data are in good agreement with the relative changes

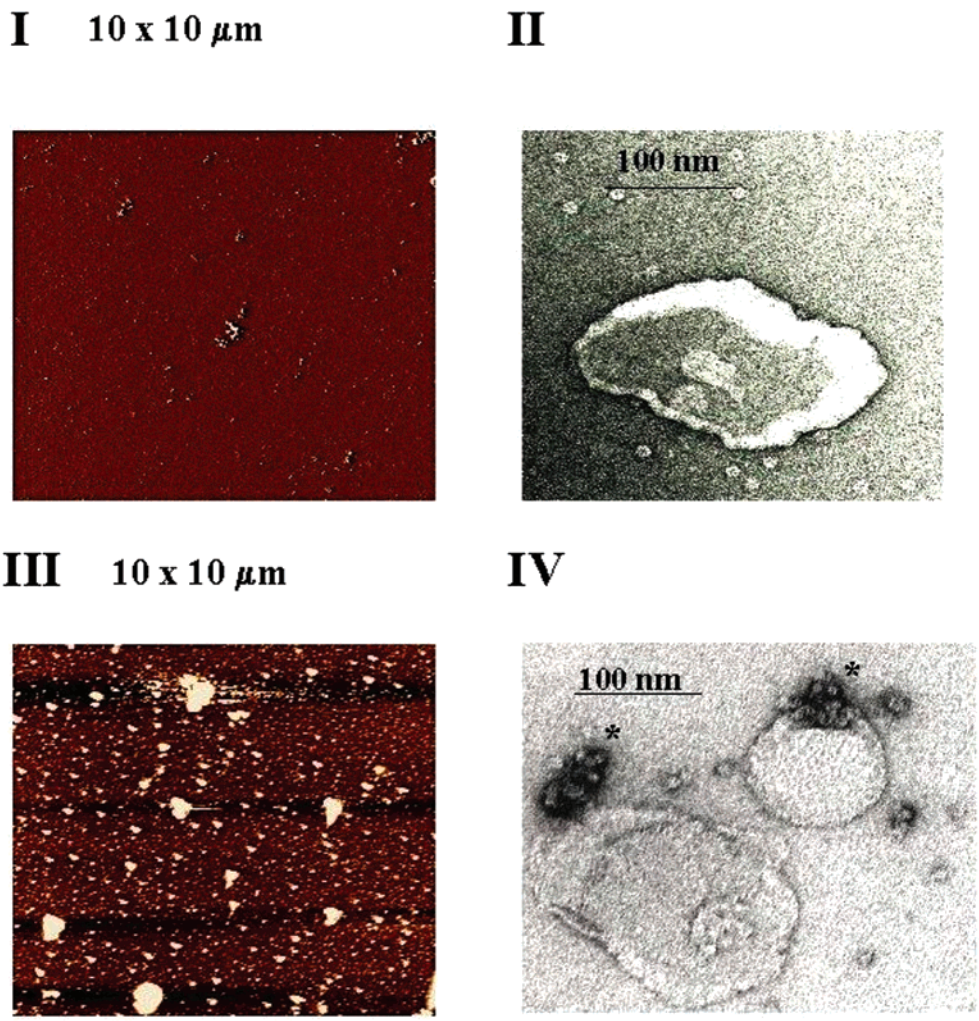

FIGURE 5: Membrane interactions of p97/p47 revealed by atomic force and electron microscopy. Monolayers are prepared from DOPE/DOPS or DOPC. Purified p97/p47 is added to the subphase, and protein/lipid films are collected onto silicon wafers (see Materials and Methods). Examinations are performed by atomic force microscopy (I, PE/PS; III, PC) and electron microscopy after negative staining (II, PE/PS; IV, PC). * denotes protein aggregates.

in hydrophobic binding pockets, probed by bisANS (Figure 6A). Changes in the secondary structure in particular are relevant to the mechanism of protein-induced membrane fusion. To reveal such overall changes, FTIR measurements, in conjunction with proton-deuterium exchange experiments were then carried out to further characterize structural changes, relevant to the mechanism of protein-induced membrane fusion.

p97/p47 Exhibits Decompaction and an Increase in α-Helical Content when Contacting PE-Containing Vesicles. After incubation of the complex for 1 h with liposomes of various compositions, unbound protein was removed by gel filtration, and the samples were analyzed for secondary structure determination by FTIR (*25*). As shown in Table 2, the α-helix and β-structure contents are about equally contributing to the main conformational features of p97/p47 in solution. After interaction with PC or PC/PS liposomes, the amide I band of p97/p47 was below detection limit, consistent with the very low amount of protein bound to such vesicles due to massive clustering (Figures 2 and 5), which either prevents proper association or causes its dissociation. Strikingly, in the presence of PE-containing vesicles, p97/p47 becomes more α-helical with less β-sheet, whereas p97 overall secondary structure remains unchanged. Note that p47 displays mainly β-structures (not shown). Thus, although both p97/p47 and p97 are able to associate with lipid vesicles containing PE (PE being a strict prerequisite for binding, see above, Figures 2 and 3), the manner in which they associate is different, leading to differences in secondary structure (see also below).

To further investigate the structural rearrangements and differences undergone by p97 alone and complexed with p47 when interacting with the vesicles, we studied the overall tertiary structure of both proteins by proton/deuterium (H/D) exchange, the state of deuteration increasing when the protein faces a hydrophilic environment (*26*). As shown in Figure 7, the exchange amounted 60 and 50% for p97 and the p97/p47 in solution, respectively. This indicates a limited accessibility of the solvent within the internal structure of these molecules. In the presence of PE-containing lipid vesicles, a rearrangement occurs, as visualized by a further increase in the accessibility of both molecules to the solvent. In the case of p97/p47, the accessibility to deuterium becomes virtually complete, since the degree of exchange amounted 90% within 2 h. This increased accessibility to deuterium suggests that their structures become less compact when interacting with PE-containing lipid bilayers, consistent with the acrylamide quenching data (Figure 6B for p97/p47).

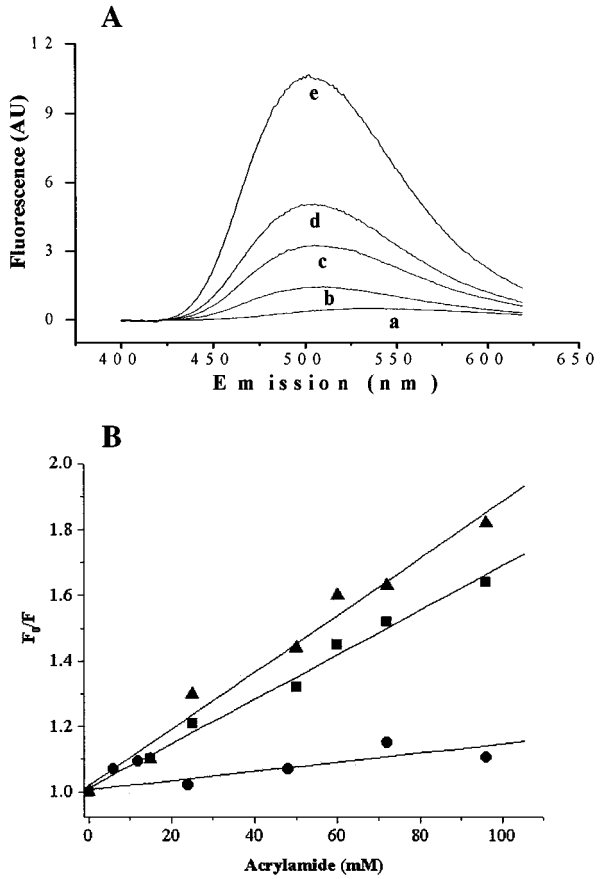

FIGURE 6: Lipid species-dependent exposure of hydrophobic sites occurs upon p97/p47/vesicle interaction. Panel A, 6 nM p97/p47 are added (b) to bisANS (60 μM) (a) in fusion buffer at 37 °C, and the emission spectrum recorded at $\lambda_{exc} = 365$ nm. Lipid vesicles (final concentration 100 μM) of PE/PS (c), PC/PS (d), or PC (e) are then added and fluorescence recorded after 3 min. Similar results were obtained when p97/p47 was added after lipid vesicles, i.e., in the presence of lipid vesicles alone, the bisANS emission spectra were reminiscent to those shown in (b). Panel B, tryptophan quenching by acrylamide. Increasing amounts of acrylamide are added to 6 nM p97/p47 in fusion buffer at 37 °C (■), in the presence of 100 μM liposomes of PE/PS (▲) or PC (●). After 3 min, fluorescence is recorded at 340 nm ($\lambda_{exc} = 295$ nm). Results are expressed as F_0/F (mean of three separate experiments), where F_0 is the fluorescence intensity in the absence and F is the fluorescence intensity in the presence of acrylamide. Data points were corrected for vesicle blank (scatter) and for the dilution caused by the acrylamide addition. Note that for both panels, the final molar protein-to-lipid ratio is 1:17 000.

Table 2: Estimates of the Secondary Structure Contents of p97 and p97/p47 in the Absence or Presence of PE/PS Vesicles

sample	α-helix[a]	β-sheet[a]	β-turn[a]
p97	47	38	15
p97 + vesicles	44	41	15
p97/p47	42	40	18
p97/p47 + vesicles	51	30	20

[a] Secondary structure determination was performed from the analysis of the shape of the amide I band using a Fourier self-deconvolution curve-fitting procedure. Final molar protein-to-lipid ratio is 1:20 000. Results are mean of three to four separate FTIR measurements, and error is within 5%. Similar results were obtained with PC/PE/PS (1:1:1) vesicles. Note that the complex does not bind to PE-devoid vesicles, which precludes any structural analysis.

To further define the relevance of these structural changes in terms of function, the effect of p97 and p97/p47 on lipid

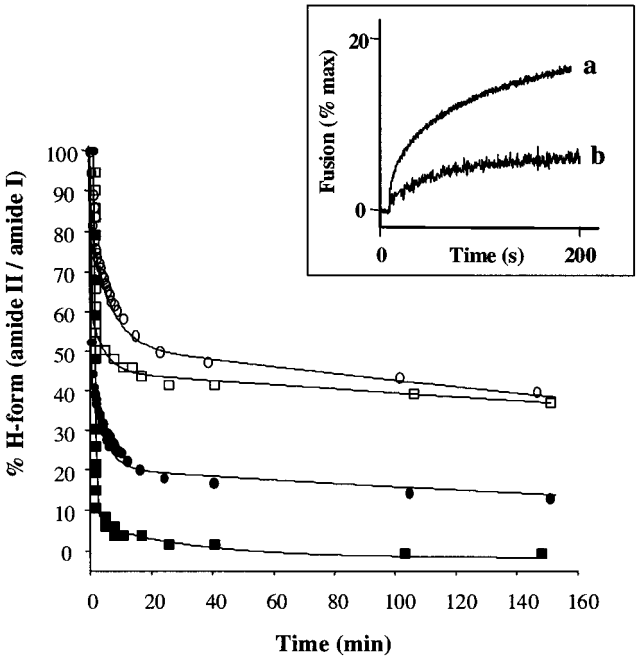

FIGURE 7: Accessibility of p97/p47 to deuterium oxide increases in the presence of PE-containing vesicles. The amide II/amide I band ratio expressed between 0 and 100% is plotted versus deuteration time. Each curve is the mean of two independent experiments. Samples are p97 (○), p97/p47 (□), p97 + PE/PS liposomes (1:1) (●), p97/p47 + PE/PS liposomes (1:1) (■). Similar results were obtained with PC/PS/PE (1:1:1) and PC/PE (1:1) liposomes, and with synthetic (dioleoyl form) or brain phospholipids. Inset, comparison of the fusion properties of p97/p47 (a) versus p97 alone (b), on PE/PS liposomes, in a 1:20 000 final molar protein-to-lipid ratio.

ordering was investigated, protein penetration being a crucial step in fusion. For PC/PS/PE (1:1:1) multilayers, in the absence of protein, the acyl chain order parameter f [at $\nu_{sym}(CH_2) \sim 2850$ cm^{-1}], calculated from polarized ATR-FTIR measurements, was 0.56. This value reflects a well-ordered phospholipid membrane. In the presence of p97, no change in the orientation of the lipid acyl chains was detectable, i.e., the value of f was 0.56. By contrast, upon interaction of the p97/p47 *complex* with the lipid vesicles, a perturbation in the organization of the bilayer occurred, corresponding to an increase in disorder with an f value of 0.27. These data thus strongly suggest that o*nly when* complexed to p47, p97 is able to embed itself (although weakly) in the lipid bilayer, whereas p97 alone cannot. Although these data can only be obtained *after* completion of the actual merging step, they are consistent with a pivotal role of protein insertion in the mechanism of membrane fusion, and signify a crucial role of p47 in regulating such a step. Considering the relative fusogenic properties of both proteins (p97 bringing about very little fusion, whereas the p97/p47 complex is highly fusogenic for concentrations as low as 5 nM, see inset to Figure 7), it may then well be that these changes in secondary structure as exhibited by p97/p47, in conjunction with changes in tertiary structure, constitute a strong prerequisite to convey fusogenic properties to the whole molecule.

DISCUSSION

Both the cytosolic ATPases NSF and p97 (*10*), in conjunction with their cofactors α-SNAP and p47, respec-

tively, and the v-and t-SNAREs (*11*) have been directly implicated in cellular fusion events. The evidence relies upon data demonstrating the ability of these proteins to mediate the fusion of postmitotic Golgi membranes (*16*), and fusion of liposomes (*10*, *11*). In contrast to the v-t-SNARE system, which fuses vesicles of a great variety of lipid compositions (*31*), the p97/p47 system shows a high degree of lipid specificity with a preference for PE-containing bilayers (*10*, this study). Such a specificity is of importance to appropriately appreciate and justify the use of liposomes as target membranes, since such membranes may display fusion susceptible to numerous proteins and peptides, irrespective of physiological relevance (see Results) (*35*). Indeed, exposure of (nonspecific) hydrophobic sequences, in conjunction with distinct structural requirements often dictate the fusion properties of "model" proteins and peptides. In that context, the careful regulation of p97/p47-induced fusion is highly relevant for the justification of the use of liposomes to probe the fusion activity of the complex. Indeed, only when mixed at an appropriate ratio the p97/p47 complex, as opposed to p97 and p47 alone, triggers fusion in an NEM- and ATP-sensitive, and lipid-dependent manner (*10*). Clearly, the biological relevance of these data is strongly supported in the present work. Here we developed an assay that allows us to monitor fusion between Golgi membranes in a cell-free system, and have thus obtained direct evidence that fusion between natural Golgi membranes triggered by p97/47 also depends on the presence of a PE-(micro) environment. These observations are therefore entirely consistent with the preference for PE previously noted in artificial systems. Indeed, a reduction in the accessible PE pool in the Golgi membrane, as accomplished by TNBS treatment or PE to PC conversion (Figure 1), resulted in a concomitant inhibition of Golgi membrane fusion. Importantly, the data also indicate that the role of PE is beyond that of merely facilitating fusion by promoting negative bilayer curvature. Rather, PE appears to provide a (micro)-environment that facilitates a controlled interaction of p97/p47 with the bilayer/water interphase, although a supportive role of charged interactions as provided by PS cannot be excluded yet. This interaction leads to gross conformational changes in the complex that enhance the *overall* α-helix content (Table 1). Interestingly, this enhancement depends on the association of p97 with its cofactor p47.

The Role of p47 in p97/p47-Induced Fusion. Although p97 alone interacts with PE-containing bilayers, only the p97/p47 complex causes disorder in the lipid acyl chain, a feature that would be consistent with (a partial) protein penetration. Furthermore, complex formation is also required for its activation to function specifically in Golgi fusion events (*8*), and our data support the view that p47 function is not merely to provide an anchorage site for p97. Indeed, the lipid binding properties of both proteins are clearly different (Figure 2), and p47 exerts a "decompacting" effect on p97 (Figures 6 and 7), as reflected by an enhancement of the surface area, interacting with the aqueous environment in the presence of lipid bilayers. p47 also inhibits the ATPase function of p97 (*36*), and thereby maintains p97 in its ATP-bound conformation, a prerequisite for mediating fusion. Interestingly, in its ATP-bound form, NSF displays extensions or "feet" (the N-terminal domain), but in the ADP-form the same domain shows a tight structuring (*37*). It is thus conceivable that p47 would maintain if not promote this extended/decompacted shape, as suggested by a higher degree of H/D exchange for the complex than for p97 (Figure 7), and by the overall "dishevelled" shape of p97/p47 observed by electron microscopy (*7*).

In vivo, the Golgi SNARE syntaxin 5 is intimately involved in the recruitment of p97/p47 (*3*). Structurally, the p97/p47/syntaxin 5 complex is arranged as a body (p97/p47) on top of two legs (syntaxin 5). p47 thus acts as linking agent between the ATPase and the SNARE, creating a membrane-anchoring point and spatially constraining the ATPase. Upon binding of p47 to a Golgi membrane (which can be considered as donor membrane), p97 could then be adequately exposed toward an acceptor Golgi membrane to pursue the fusion step. In the presence of PE-rich acceptor membranes, p47 further modulates the shape of p97: the complex displays an *overall* increase in helicity (Table 2), with the exposure of previously buried hydrophobic "pockets" (Figure 6A). This leads to efficient membrane association (Figure 2), to further decompaction through changes in tertiary structure (Figure 7), and to alteration in bilayer organization through protein−lipid interaction. Ultimately fusion occurs, which is consistently much higher for p97/p47 than for p97 (inset to Figure 7). Indeed, p97 as such shows no α-helical change, remains more compact, and does not penetrate, as suggested by its inability to change acyl chain ordering. Thus, p47 modulates the structure of p97 in a way promoting overall structural changes, apparently relevant to the expression of the fusion function. Presumably, the overall structural changes directly or indirectly affect a fusion domain located in p97/p47, leading to a modulation of the fusion activity.

The Role of PE in p97/p47-Induced Fusion. In the Golgi−Golgi fusion assay, p97/p47-induced fusion is prominently affected by modifications of the PE pool (Figure 1). However, other lipids also exert an effect on p97/p47 structure, most notably PC; yet, only PE induces changes relevant to the fusion step. Remarkably, extensive PC-mediated clustering of the complex occurs on mono- or bilayer surfaces (Figures 5 and 6) through hydrophobic protein−protein interactions arising from protein−lipid interactions. Hydrophobic interaction of these clusters to membranes is inefficient (Figure 5, III, IV), explaining the lack of recovery of the complex interacting with PE-devoid bilayers after gel filtration and sucrose gradient centrifugation (Figure 2). Consequently, in conjunction with a tightening of headgroup spacing, such complexes very likely trigger little if any fusion (Figure 4, Table 1).

In the presence of PE, a more subtle structural reorganization occurs within the complex, resulting in a less compacted structure (Figures 6B and 7). Since the complex shows a homogeneous distribution on PE-containing monolayers (Figure 5, I, II), it appears that protein−lipid rather than protein−protein interactions are promoted at these conditions, which translates into efficient vesicle binding (Figure 2). The structural flexibility underlying the decompaction may well be required for the exposure of (a) domain(s) that embed(s) into the target bilayer. This embedment is further facilitated by the spacing effect of PE on headgroups (Figure 4), and gives rise to a local increase in disorder, preceding the ultimate membrane fusion step (Figure 7). Hence, these data would be fully consistent with the notion that (a) domain(s)

of p97/p47 enter(s) the lipid hydrocarbon core, which is *not* observed for p97. However, the nature and position of this domain into the complex remain unknown at present.

The prominent role of PE is further emphasized by the notion that PS, another prominent lipid in Golgi membranes, cannot overtake its role in promoting complex interaction with PC-containing bilayers and subsequently fusion (Figure 2, Table 1). However, substitution of part of the PC by PS in the mixed PE/PC bilayer further increases the rate of fusion (Table 1). This might be because a decrease in PC content may favor p97/p47 interaction with the PC/PS/PE bilayer, compared to PC/PE. Alternatively, it is also possible that a reduction in membrane-bound water (PC being the most strongly hydrated lipid) could have given rise to a decrease in intermembrane hydration repulsion, which also could promote fusion (Table 1).

Clearly, however, the presence of PE is required for the interaction of p97/p47 with membranes, and the role of PE and PC in the structural modulation of the complex indicates an additional dimension, i.e., other than in terms of hydration repulsion, of these lipids in p97/p47-mediated membrane fusion.

Our data indicate that the transition between nonfusogenic and fusogenic states of the complex is related to subtle protein−lipid interactions in the ATP-bound state (*10*, *16*), and a modulation by lipids of p97/p47-induced Golgi membrane fusion in vivo is realistic. Moreover lipid-induced conformational changes relevant to fusion have been recently documented (*23*). Fusion peptides can penetrate the target bilayer as amphipathic α-helices (*38*, *39*). By analogy, it is tempting to speculate that the domain(s) of p97/p47 that embed(s) into the lipidic core is itself α-helical. This would be consistent with the observed increase in helicity, and with p97 showing no change in helicity nor the capacity to disorder acyl chains. It will be of interest to determine whether this lipid-interacting domain may bear similarities to the lipid-binding domain recently determined in Vps4p, a member of the AAA-ATPase family to which p97 belongs (*40*, *41*). Comparison of the primary sequence of the Vps4p 30-residue domain with that of p97 reveals striking similarities. In p97/p47, p47 could therefore optimally modulate the "presentation" of that domain toward the target membrane, to trigger changes required for expressing membrane fusion. The use of peptides with the corresponding sequence of that region or of mutants of the now available bacterially expressed p97, combined with recombinant p47, could prove useful to test this tempting hypothesis.

In conclusion, this is the first demonstration that the cytosolic p97/p47 complex, when contacting target membranes, undergoes PE-dependent overall conformational changes. Among others, these changes lead to membrane perturbations that likely involve the penetration of (a) domain(s) into the lipid bilayer. In a complex-specific manner, membrane fusion is triggered, the PE microenvironment dependence of which was demonstrated in a pure Golgi membrane fusion assay, which emphasizes the physiological significance of the present work.

ACKNOWLEDGMENT

We thank Drs. Jean Vance for helpful suggestions, Martin Latterich for providing antibodies and purified p97, Marlies Otter-Nilsson for purified p97/p47 complex, and Wilma Bergsma for help in electron microscopy.

REFERENCES

1. Acharya, U., Jacobs, R., Peters, J. M., Watson, N., Farquhar, M. G., and Malhotra, V. (1995) The formation of Golgi stacks from vesiculated Golgi membranes requires two distinct fusion events. *Cell 82*, 895−904.
2. Rabouille, C., Levine, T. P., Peters, J. M., and Warren, G. (1995) An NSF-like ATPase, p97, and NSF mediate cisternal regrowth from mitotic Golgi fragments. *Cell 82*, 905−914.
3. Rabouille, C., Kondo, H., Newman, R., Hui, N., Freemont, P., and Warren, G. (1998) Syntaxin 5 is a common component of the NSF- and p97-mediated reassembly pathways of Golgi cisternae from mitotic Golgi fragments in vitro. *Cell 92*, 603−610.
4. Warren, G., and Malhotra, V. (1998) The organisation of the Golgi apparatus. *Curr. Opin. Cell Biol. 10*, 493−498.
5. Whiteheart, S. W., Brunner, M., Wilson, D. W., Wiedmann, M., and Rothman, J. E. (1992) Soluble *N*-ethylmaleimide-sensitive fusion attachment proteins (SNAPs) bind to a multi-SNAP receptor complex in Golgi membranes. *J. Biol. Chem. 267*, 12239−12243.
6. Steel, G. J., Buchheim, G., Edwardson, J. M., and Woodman, P. G. (1997) Evidence for interaction of the fusion protein α-SNAP with membrane lipid. *Biochem. J. 32*, 511−518.
7. Kondo, H., Rabouille, C., Newman, R., Levine, T. P., Pappin, D., Freemont, P., and Warren, G. (1997) p47 is a cofactor for p97-mediated membrane fusion. *Nature 388*, 75−78.
8. Meyer, H. H., Shorter, J. G., Seemann, J., Pappin, D., and Warren, G. (2000) A complex of mammalian Ufd1 and Npl4 links the AAA-ATPase, p97, to ubiquitin and nuclear transport pathways. *EMBO J. 19*, 2181−2192.
9. Patel, S. K., Indig, F. E., Olivieri, N., Levine, N. D., and Latterich, M. (1998) Organelle membrane fusion: a novel function for the syntaxin homologue Ufe1p in ER membrane fusion. *Cell 92*, 611−620.
10. Otter-Nilsson, M., Hendriks, R., Pécheur-Huet, E. I., Hoekstra, D., and Nilsson, T. (1999) Cytosolic ATPases, p97 and NSF, are sufficient to mediate rapid membrane fusion. *EMBO J. 18*, 2074−2083.
11. Weber, T., Zemelman, B. V., McNew, J. A., Westermann, B., Gmachi, M., Parlati, F., Söllner, T., and Rothman, J. E. (1998) SNAREpins: minimal machinery for membrane fusion. *Cell 92*, 759−772.
12. Mayer, A. (1999) Intracellular membrane fusion: SNAREs only? *Curr. Opin. Cell Biol. 11*, 447−452.
13. Peters, C., Bayer, M. J., Buhler, S., Andersen, J. S., Mann, M., and Mayer, A. (2001) Trans-complex formation by proteolipid channels in the terminal phase of membrane fusion. *Nature 409*, 581−588.
14. Ungermann, C., Sato, K., and Wickner, W. (1998) Defining the functions of *trans*-SNARE pairs. *Nature 396*, 543−548.
15. Ungermann, C., Nichols, B. J., Pelham, H. R. B., and Wickner, W. (1998) A vacuolar v-t-SNARE complex, the predominant form in vivo and on isolated organelles, is disassembled and activated for docking and fusion. *J. Cell Biol. 140*, 61−69.
16. Müller, J. M. M., Rabouille, C., Newman, R., Shorter, J., Freemont, P., Schiavo, G., Warren, G., and Shima, D. T. (1999) An NSF function distinct from ATPase-dependent SNARE disassembly is essential for Golgi membrane fusion. *Nature Cell Biol. 1*, 335−340.
17. Slusarewicz, P., Nilsson, T., Hui, N., Watson, R., and Warren, G. (1994) Isolation of a matrix that binds medial Golgi enzymes. *J. Cell Biol. 124*, 405−413.
18. Stuart, R. A., Mackay, D., Adamczewski, J., and Warren, G. (1993) Inhibition of intra-Golgi transport in vitro by mitotic kinase. *J. Biol. Chem. 268*, 4050−4054.
19. Takahashi, S., Yamamura, T., Kamo, M., and Satake, K. (1984) Regeneration of amino compounds from the 2,4,6-trinitrophenyl derivatives by treatment with hydrazine. *Chem. Lett.* 127−130.
20. Vance, J. E., and Vance, D. E. (1988) Does rat liver Golgi have the capacity to synthesize phospholipids for lipoprotein secretion? *J. Biol. Chem. 263*, 5898−5909.
21. Waterfield, C. J., Asker, D. S., and Timbrell J. A. (1997) Triglyceride disposition in isolated hepatocytes after treatment with hydrazine. *Chem. Biol. Interact. 107*, 157−172.

22. Slater, S. J., Kelly, M. B., Taddeo, F. J., Ho, C., Rubin, E., and Stubbs, C. D. (1994) The modulation of protein kinase C activity by membrane lipid bilayer structure. *J. Biol. Chem. 269*, 4866−4871.
23. Pécheur, E. I., Martin, I., Bienvenüe, A., Ruysschaert, J. M., and Hoekstra, D. (2000) Protein-induced fusion can be modulated by target membrane lipids through a structural switch at the level of the fusion peptide. *J. Biol. Chem. 275*, 3936−3942.
24. Hoekstra, D., and Klappe, K. (1993) Fluorescence assays to monitor fusion of enveloped viruses. *Methods Enzymol. 220*, 261−276.
25. Goormaghtigh, E., Raussens, V., and Ruysschaert, J. M. (1999) ATR-FTIR spectroscopy of proteins and lipids in biological membranes. *Biochim. Biophys. Acta 1422*, 105−185.
26. De Jongh, H. H., Goormaghtigh, E., and Ruysschaert, J. M. (1996) The different molar absorptivities of the secondary structure types in the amide I region: an attenuated total reflection infrared study on globular proteins. *Anal. Biochem. 242*, 95−103.
27. Gosh, J. M., Peisajovich, S. G., Ovadia, M., and Shai, Y. (1998) Structure−function study of a heptad repeat positioned near the transmembrane domain of sendai virus fusion protein which blocks virus-cell fusion. *J. Biol. Chem. 273*, 27182−27190.
28. Oberle, V., Bakowsky, U., Zuhorn, I. S., and Hoekstra, D. (2000) Lipoplex formation under equilibrium conditions reveals a three-step mechanism. *Biophys. J. 79*, 1447−1454.
29. Cayot, P., and Tainturier, G. (1997) The quantification of protein amino groups by the trinitrobenzenesulfonic acid method: a reexamination. *Anal. Biochem. 249*, 184−200.
30. Yang, C. C., and Chang, L. S. (1989) Studies on the status of lysine residues in phospholipase A2 from Naja naja atra (Taiwan cobra) snake venom. *Biochem. J. 262*, 855−60.
31. Brügger, B., Nickel, W., Weber, T., Parlati, F., McNew, J. A., Rothman, J. E., and Söllner, T. (2000) Putative fusogenic activity of NSF is restricted to a lipid mixture whose coalescence is also triggered by other factors. *EMBO J. 19*, 1272−1278.
32. Van Meer, G. (1998) Lipids of the Golgi membrane. *Trends Cell Biol. 8*, 29−33.
33. Pécheur, E. I., Sainte-Marie, J., Bienvenüe A., and Hoekstra D. (1999) Lipid headgroup spacing and peptide penetration, but not peptide oligomerization, modulate peptide-induced fusion. *Biochemistry 38*, 364−373.
34. Hoekstra, D., Buist-Arkema, R., Klappe, K., and Reutelingsperger, C. P. M. (1993) Interaction of annexins with membranes: the N-terminus as a governing parameter as revealed with a chimeric annexin. *Biochemistry 32*, 14194−14202.
35. Pécheur, E. I., Sainte-Marie, J., Bienvenüe, A., and Hoekstra, D. (1999) Peptides and membrane fusion: towards an understanding of the molecular mechanism of protein-induced fusion. *J. Membr. Biol. 167*, 1−17.
36. Meyer, H. H., Kondo, H., and Warren, G. (1998) The p47 cofactor regulates the ATPase activity of the membrane fusion protein, p97. *FEBS Lett. 437*, 255−257.
37. Hanson, P. I., Roth, R., Morisaki, H., Jahn, R., and Heuser, J. (1997) Structure and conformational changes in NSF and its membrane receptor complexes visualized by quick-freeze/deep-etch electron microscopy. *Cell 90*, 523−535.
38. Han, X., Bushweller, J. H., Cafiso, D. S., and Tamm, L. K. (2001) Membrane structure and fusion-triggering conformational change of the fusion domain from influenza hemagglutinin. *Nat. Struct. Biol. 8*, 715−720.
39. Martin, I., Pécheur, E. I., Ruysschaert, J. M., and Hoekstra D. (1999) Membrane fusion induced by a short fusogenic peptide is assessed by its insertion and orientation into target bilayers. *Biochemistry 38*, 9337−9347.
40. Babst, M., Wendland, B., Estepa, E. J., and Emr, S. D. (1998) The Vps4p AAA ATPase regulates membrane association of a Vps protein complex required for normal endosome function. *EMBO J. 17*, 2982−2993.
41. Bishop, N., and Woodman, P. (2000) ATPase-defective mammalian VPS4 localizes to aberrant endosomes and impairs cholesterol trafficking. *Mol. Biol. Cell. 11*, 227−239.

BI0259195